frontiers | Frontiers in Materials

TYPE Review
PUBLISHED 26 January 2023
DOI 10.3389/fmats.2023.1135864

OPEN ACCESS

EDITED BY
Wei Qin,
Changsha University of Science and Technology, China

REVIEWED BY
Huai-Jun Lin,
Jinan University, China
Claudia Zlotea,
Centre National de la Recherche Scientifique (CNRS), France
Jacques Huot,
Université du Québec à Trois-Rivières, Canada

*CORRESPONDENCE
Di Wan,
di.wan.rwth@gmail.com

†Present address:
Di Wan,
School of Materials Science and Engineering, Beijing Institute of Technology, Beijing, China; Advance Research Institute of Multidisciplinary Science, Beijing Institute of Technology, Beijing, China

SPECIALTY SECTION
This article was submitted to Energy Materials, a section of the journal Frontiers in Materials

RECEIVED 02 January 2023
ACCEPTED 17 January 2023
PUBLISHED 26 January 2023

CITATION
Kong L, Cheng B, Wan D and Xue Y (2023), A review on BCC-structured high-entropy alloys for hydrogen storage.
Front. Mater. 10:1135864.
doi: 10.3389/fmats.2023.1135864

A review on BCC-structured high-entropy alloys for hydrogen storage

Lingjie Kong[1,2], Bo Cheng[1,2], Di Wan[3*†] and Yunfei Xue[1,2]

[1]School of Materials Science and Engineering, Beijing Institute of Technology, Beijing, China, [2]Yangtze Delta Region Academy of Beijing Institute of Technology, Jiaxing, Zhejiang, China, [3]Department of Mechanical and Industrial Engineering, Norwegian University of Science and Technology, Trondheim, Norway

Recently, high entropy alloys (HEAs) with body-centred cubic (BCC) single phase structures have attracted wide attention in many fields including hydrogen storage, due to their unique structural characteristics and excellent performance. Its novel design concept provides more possibilities for the investigation of advanced hydrogen storage materials, in which several remarkable research works have been published, providing opportunities for the design of hydrogen storage materials with unprecedented properties. In this review, we combed through the definition and criteria of high entropy alloys, and summarized the current research status of body-centred cubic-structured high entropy alloys for hydrogen storage from multiple perspectives of composition designs, synthesis processes, and hydrogen storage properties. Moreover, the possible application scenarios and future research directions are analysed.

KEYWORDS

high entropy alloys, BCC, solid-state hydrogen storage, hydrogen storage capacity, kinetics, thermodynamics

1 Introduction

As an ideal energy carrier and secondary clean energy source, hydrogen shows great prospective in the fields of transportation, industrial fuel and power energy storage owing to its high combustion calorific value and non-polluting characteristics (Lebrouhi et al., 2022). The development of the hydrogen energy industry will serve as crucial strategic pillars in driving the global energy transition and meeting decarbonization targets (Lebrouhi et al., 2022; Zhao et al., 2022). The hydrogen energy industry chain can be broadly categorised into three parts: hydrogen production, hydrogen storage and transportation, hydrogen application. With the number of policies and projects regarding the hydrogen energy industry expanding rapidly, the safe and efficient hydrogen storage technology has become an essential challenge towards the application of hydrogen at scale. Hydrogen storage can be realized in the state of gas, liquid or solid. Storing hydrogen *via* high-pressure tanks (~70 MPa) is currently the most commercially mature method available, but the accompanying safety hazards cannot be ignored (Rohit et al., 2022). Liquid hydrogen, despite its high energy load, requires extremely high maintenance power and is therefore more limited to aerospace applications (Usman, 2022). Solid-state storage techniques in the form of metal hydrides with high volumetric hydrogen density and security have appeared as attractive alternatives (Kumar et al., 2022).

Metal hydride, utilising a reversible chemical interaction of hydride-forming alloys, is the primary focus of the solid-state hydrogen storage community. Researches on these materials have focused on the development of potential candidates with improved bulk

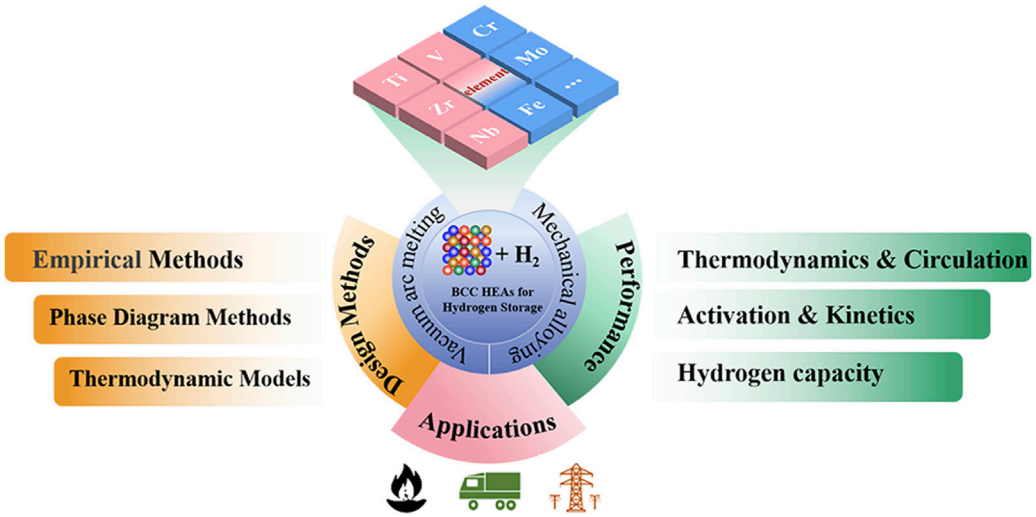

FIGURE 1
Diagram showing the design, synthesis, hydrogen storage properties and applications of BCC-structured HEAs.

and weight capacities, kinetics of rapid hydrogen desorption, and long-term cycling stability (Rusman and Dahari, 2016). In promising alloy systems, rare earth-based alloys show excellent potential as they possess favourable room temperature reversible hydrogen absorption/desorption properties and long-term cycling stability (Dashbabu et al., 2022; Lv et al., 2022), but are more restricted to Ni-MH battery applications due to their low hydrogen storage capacity (Liu et al., 2004). Constrained by the difficulty of activation and sensitivity to impurities, TiFe-based alloys are only the candidates for hydrogen compressor and vehicle applications, despite their low price and fairly low hydrogenation temperature (Peng et al., 2021; Li et al., 2022; Liu et al., 2022a; Zhang et al., 2022). The unique advantages of Mg-based alloys in terms of a high hydrogen storage capacity make them a strong contender for vehicle-mounted hydrogen storage materials. Low cost and naturally abundant resources make it possible to scale-up the application of Mg-based alloys, however, the fact that hydrogenation reactions are limited to high temperatures is the biggest obstacle to their practical application, and the slow kinetic properties are also a challenge that cannot be ignored (Yin et al., 2018). Solid-solution alloys (especially V-based alloys) exhibit diverse property tuning and have a wider range of applications. The equilibrium between hydrogen storage performance and hydrogen storage conditions is the primary objective for developing new hydrogen storage materials. There are also some alloys with sub-stable structures that have been reported as hydrogen storage materials, and a review and outlook on such new systems of hydrogen storage alloys is presented by Lin et al. (2022). Among them, high-entropy alloys show unique advantages for hydrogen storage.

High entropy alloys (HEAs), a new alloying strategy with high concentration of multi-principal elements, is expected to enable hydrogen storage performance compatible with hydrogen storage conditions because of its diverse composition, designable phase structure and unique hydrogen performance, especially the proposed concept of single phase HEAs which might provide a brand new inspiration for clarifying the mechanism of hydrogen storage. A growing number of reports suggest that body-centred cubic (BCC)-structured HEAs exhibit better hydrogen storage properties (hydrogen capacity, kinetics, activation and cyclability, etc.) than conventional alloys (Sahlberg et al., 2016; Zhang et al., 2020; Sleiman and Huot, 2021). The composition design and preparation process of these alloys can also have a significant influence on its properties for different hydrogen applications. Although several reviews on high-entropy hydrogen storage alloys have been published, a comprehensive report on BCC-structured HEAs for hydrogen storage is still lacking.

In this paper, the latest research results of HEAs with BCC structure for hydrogen storage are investigated. The preparation of these alloys and their theoretical criteria are briefly mentioned, followed by a compositional design approach based on the reaction of hydrogen with a multi-principal element alloy. Various aspects of hydrogen storage performance (capacity, activation, kinetic properties and cyclability) are described in detail and the potential applications are discussed, as can be seen in Figure 1. This work will contribute to the design and development of single phase HEAs for hydrogen storage.

2 Concept and design of HEAs

2.1 Definitions and criteria

The concept of HEAs was published in 2004 and was defined as alloys containing at least five major elements with 5%–35% atomic fraction of each element, which were considered to have a mixing entropy at high temperatures sufficient to overcome the formation enthalpy of the intermetallic phase ($\Delta S_{conf} > 1.5R$) and obtain a stable solid-solution structure (Yeh et al., 2004). However, some ternary and quaternary alloys were reported to have similar properties, and thus the definitions of HEAs seem to

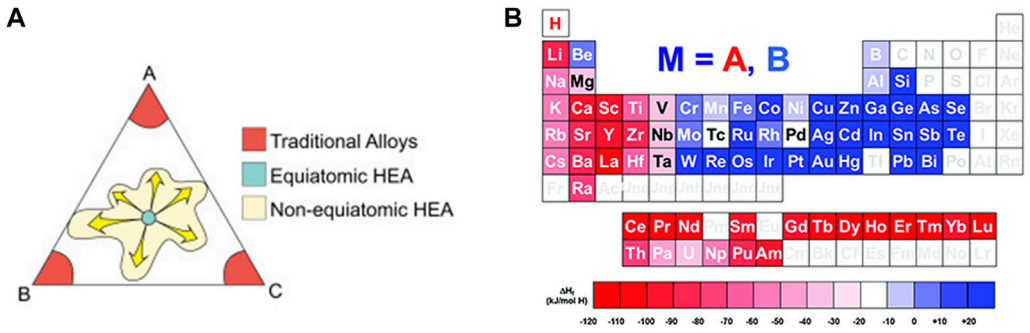

FIGURE 2
Comparison of the positions of high entropy alloys and conventional alloys on the isothermal cross section of the ternary phase diagram **(A)** (Pradeep et al., 2015); the relative division of hydrogen-absorbing (in red) and non-hydrogen-absorbing (in blue) elements in the periodic table of elements according to the enthalpy of formation of M-H metal hydrides **(B)** (Latroche et al., 2021).

be inaccurate (Senkov et al., 2010; Senkov et al., 2013; Guo et al., 2013). Subsequently, the concept of multi-principal element alloys reported in the same year started to be accepted by the growing number of academics (Cantor et al., 2004), relying on this concept opening up a new and unexplored region of alloy composition. Actually, the definitions of HEAs are only approximate guidelines and not strictly laws, and an increasing number of single phase multi-principal element alloy systems have stimulated intense interest among researchers.

Theoretical design methods for multi-principal element high entropy alloying generally rely on empirical parameter criteria such as atomic size (δ), mixing entropy/enthalpy ($\Delta H_{\mathrm{mix}}/\Delta S_{\mathrm{mix}}$), valence electron concentration (VEC), and some inferred parameters to predict whether the alloy can form a solid solution phase. Zhang et al. (2008) suggested that multi-principal element alloys tend to form solid solution phases when the atomic radius difference $\delta < 6.5\%$, the mixing enthalpy is limited to −15~−5 kJ/mol and the mixing entropy is limited to 12–17.5 J/(K-mol). Guo et al. (2011) have proposed the VEC criterion which suggests that the face-centred cubic (FCC) solid solution phase is more stable for VEC > 8.6 and the BCC solid solution phase is more stable for VEC < 6.87. However, these ideas are built upon the basis that the solid solution phase can be formed in the alloy and cannot be used as a criterion for the formation of HEA phase structures. These studies have shown that using δ, ΔH_{mix}, and ΔS_{mix} as independent criteria has flaws and cannot characterize the solid solution phase formation pattern. Therefore, a new parameter Ω was introduced to represent the thermodynamic stability of the multi-principal element disordered solid solution for a given temperature (Yang et al., 2014), which shows that the solid solution is relatively stable for $\Omega(T) > 1$. The specific expression of the parameter $\Omega(T)$ is given by the following equation.

$$\Omega(T) = \frac{T\Delta S_{mix}}{|\Delta H_{mix}|} \tag{1}$$

where T is the thermodynamic temperature; ΔH_{mix} is the mixing enthalpy and ΔS_{mix} is the mixing entropy. These criteria based on empirical parameters are simply effective in predicting the formation of solid solutions in alloys, especially the Ω criterion. Utilization of these criteria can avoid to some extent the material wastage caused by blind alloy preparation.

2.2 Design strategy of BCC structure HEAs: Theory and calculation method

The design of alloy composition for hydrogen storage should be focused on element-hydrogen interactions, on which appropriate hydride forming element coordination has a significant impact. HEAs pay attention to the elements at the centre of a phase diagram, as shown in Figure 2A, expanding the range of compositional choices (Pradeep et al., 2015).

The design of BCC-structured HEAs for hydrogen storage usually follows the complementarity of the different elements and thus an approximate range of element selection can be determined. To ensure the formation of the solid solution phase, these elements should meet the criteria of atomic size difference $\delta < 6.5\%$ and parameter $\Omega > 1$. Considering the hydrogen storage properties for different applications, a combination between hydrogen-absorbing elements (lower enthalpy of hydride formation and higher hydrogen affinity) and non-hydrogen-absorbing elements (higher enthalpy of hydride formation and lower hydrogen affinity) is generally required. Figure 2B shows the division of the two types of elements in the periodic table (Latroche et al., 2021). Within this scope, empirical and computational methods are proposed.

The design from empirical parameter criteria was widely used. Nygård demonstrated that the hydrogen storage properties of the alloy can be predicted from the VEC: a lower hydrogen desorption temperature corresponds to a higher VEC, because the thermal stability of hydride is influenced by the VEC. While Nygård also suggested that VEC can be helpful for predicting the hydrogen storage capacity in the design of HEA and considered VEC = 5.0 as the hydrogen capacity threshold (Nygård et al., 2019a). Zlotea et al. (2022) presented a detailed design range of 1.1–1.35 H/M for VEC > 4.9 and 1.5–2.0 H/M for VEC ≤ 4.9. Moreover, Edalati et al. (2020) suggested that the rapid hydrogen absorption/desorption performance can be obtained at room temperature when the VEC is greater than 6.4. In our work (Cheng et al., 2022), TiVNbCr alloys with different VECs were designed and it was discovered that they possess a hydrogen capacity of H/M = 2 for a widely range of compositions, reaching a high

hydrogen capacity of 3.7 wt%. Nygård et al. (2020) suggested that altered H occupation behaviour is responsible for VEC affecting hydrogen storage performance, however, Silva's research directed VEC to the effect on the thermodynamics of hydride formation, considering the change in desorption performance to be multifactorial (Silva et al., 2021). This result seems to indicate that there are limitations in the usage of empirical methods, therefore a more cautious consideration is needed for empirical methods to guide composition design. The atomic mismatch degree is likewise considered as a compositional design method. In previous reports, Shen et al. (2020) designed TiZrHfNbMo alloys with different unit cell sizes by adding different Mo contents, showing that small unit cells are more beneficial for hydride decomposition. And the cell variation due to atomic mismatch degree δ_r was considered to be uncorrelated with the hydrogen capacity in Nygård's report (Nygård et al., 2019b). This was also confirmed by Ek in the TiVZrNbHf system (Ek et al., 2021). Empirical parameters (especially VEC) are recognized to help design HEA compositions for hydrogen storage, but the applicability range as mentioned above and the low accuracy of performance predictions are the major challenges. Another core issue is that the empirical parameters ignore the influence of other factors, and the impact of empirical parameters on the performance may be diminished as the composition becomes more sophisticated. Thus a higher precision and more comprehensive design methods are needed for HEAs for hydrogen storage.

The computational phase diagram (CALPHAD model) guides the design by calculating the phase equilibrium relationship of the system based on thermodynamic parameters. Database construction, which is the basis for predicting phase equilibria of multi-component alloys, has become the focus of designing new hydrogen storage alloys. The phase structure prediction of HEAs relies on extrapolation, which is accomplished because the current database is primarily constructed from thermodynamic evaluations of simple metal-hydrogen systems (pure elemental, binary and ternary), but a great match between predictions and experimental results has been reported. Strozi et al. (2022) designed compositions with different phase structures (BCC and C15 Laves phases) in the TiVNbCr system through the CALPHAD method, and excellent prediction accuracy was demonstrated by X-ray diffraction (XRD) for the different phase structures. Following the same strategy, we designed three compositions of TiVNbCr system with BCC single phase by CALPHAD approach, and the XRD experiments demonstrated the phase diagram prediction with high accuracy (Cheng et al., 2022). As the application demands increase, the design approach to theoretical calculations is extended. Computational methods such as density functional theory (DFT) play an important role in predicting hydrogen storage properties for HEA design. Hu et al. (2019) designed a BCC single phase TiZrHfScMo alloy, which is predicted to stably accommodate 2.14 wt% H based on DFT calculations. Following this, Hu et al. (2021a) evaluated the hydrogen storage properties of TiZrVMoNb alloy, in which the important factors affecting the hydride stability were reported, which contributed significantly to the design of alloys with high reversible hydrogen storage capacity.

Computational approach is promising for implementing composition design based on hydrogenation performance requirements. Zepon et al. (2021) developed a thermodynamic model for calculating pressure-composition-isotherm (PCT) curves of multi-principal element metal-H systems. The model describes the mixing entropy with the aid of the ideal configurational entropy of interstitial solid solutions and the entropy model with site blocking effect proposed by Garcés (2010), while the enthalpy of mixing is approximated through experimental and DFT calculation data. The calculated results exhibit two plateau regions, which correspond to the stages of the phase transition for hydrogen absorption in BCC alloys, and it demonstrates a match with the experimental results for BCC structure alloys, as shown in Figure 3. The model allows the rapid selection of alloy compositions that meet the hydrogen storage requirements (e.g., capacity, plateau pressure) and the prediction of the hydrogen absorption and desorption performance of HEAs. It should be noticed that the model describes the thermodynamic parameters by using approximations, and the accuracy of the calculation can be further improved when the parameters are adjusted. Witman et al. (2021) reported another method for the thermodynamic calculations of HEAs, a machine/statistical learning (ML) model. This work is a reduction of the time consumption for first-principles modelling and experimental validation, which could rapidly filter valuable combinations of elements to obtain the predicted performance. The authors screened several components in the BCC HEA system that exhibit significant instability in hydride equilibrium pressure through an improved ML model (extended training set), with a 70-fold increase relative to hydride $TiVZrNbHfH_x$ equilibrium pressure. Although this ML model currently supports only thermodynamic property prediction, the DFT approach can help analyse alloy hydrogenation capabilities. It is suggested that when more ML training data are made available, the discovery of compositional combinations that simultaneously exhibit thermodynamic instability without sacrificing capacity over a wider HEA composition space is potentially achievable.

Empirical parameters (e.g., VEC, atomic mismatch) are used to guide the compositional design, but there are certain deficiencies considering the vast range of HEAs for hydrogen storage. The complex and lengthy experimental validation process limits the exploration of effective compositions. Using computational tools to simulate and predict the thermodynamic properties has become an attractive option, which has the advantage of quickly screening the thermodynamic properties of a large number of element combinations based on the target properties. Those models can further enhance the extent and accuracy of predictions in conjunction with the thermodynamic calculations (DFT methods). Thus, it is suggested that the future composition design of high-entropy hydrogen storage alloys should be relying on computational methods as it enables saving significant experimental costs.

3 Synthesis of BCC-structured HEAs

The synthesis process of BCC-structured HEAs can be classified as: melting and casting, mechanical alloying and powder metallurgy, according to the existing research and application experience. It is basically the same as that of conventional structure alloys, but also with special features to ensure their single-phase structure.

The melting and casting method is usually performed under a protective atmosphere, which is used to protect the alloys from oxidation during the melting process as well as the introduction of impurities. Vacuum arc melting (VAM) is a commonly used synthesis method for HEAs in the hydrogen storage community. It utilizes the arc heat generated by the discharge between electrodes to rapidly heat

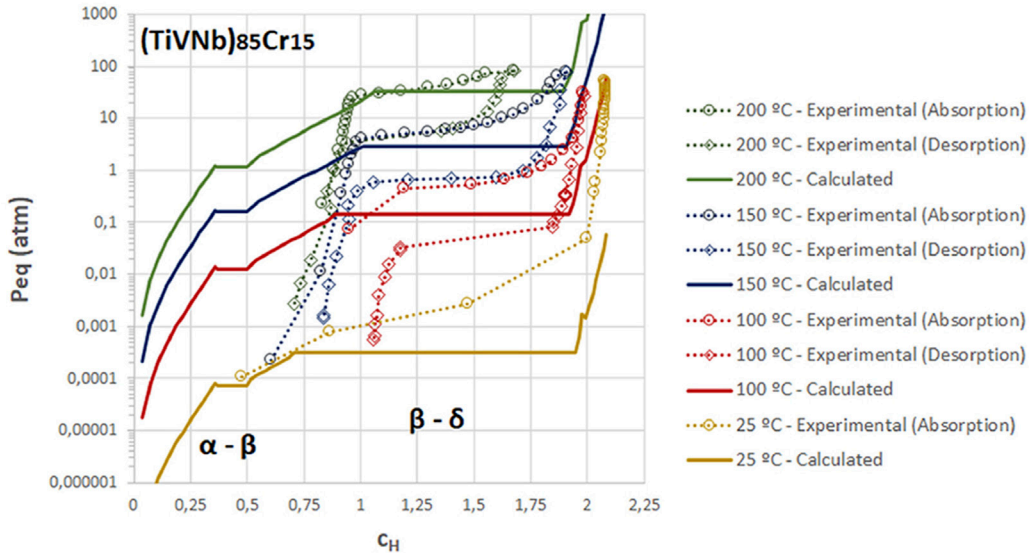

FIGURE 3
Comparison between calculated and experimental PCT curves for $(TiVNb)_{85}Cr_{15}$ at different temperatures (Zepon et al., 2021).

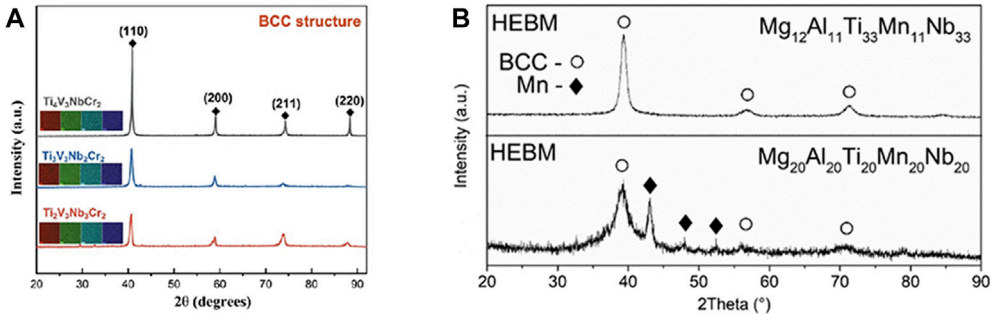

FIGURE 4
XRD patterns of the TiVNbCr system alloy synthesized by the VAM method **(A)** (Cheng et al., 2022); and XRD patterns of $Mg_{12}Al_{11}Ti_{33}Mn_{11}Nb_{33}$ HEA synthesized by the HEBM method **(B)** (Strozi et al., 2021a).

the raw materials to the molten state and remove some volatile impurities, while the uniformity of the composition can be ensured (remelting ≥ 5 times). The fused alloy liquid is then cooled and solidified in the copper crucible to obtain the HEA lump. Wang (2009) reported that the VAM method is more favourable to form the BCC structure and to maintain the hydrogen storage capacity of the alloy. The VAM method has also been used in several of our works to synthesize alloys that maintain a good single-phase structure (the alloy structure is presented in Figure 4A) (Cheng et al., 2022). Based on the above advantages, VAM has become a more popular synthesis method for BCC HEAs for hydrogen storage.

Mechanical alloying (MA) is another synthesis technology to achieve atomic level alloying between elements by subjecting metal powders to repeated deformation, cold welding, and crushing through ball milling, also referred to as high-energy ball milling technology (HEBM). Varalakshmi et al. (2008) published about the preparation of AlFeTiCrZrCu HEA by HEBM in 2008, and the work suggested that the alloy powder could form a uniform single BCC structured solid solution after 20 h of HEBM. Mg-based HEAs for hydrogen storage domain can also be alloyed. Zepon et al. (2017) confirmed the feasibility of this approach by synthesizing $MgZrTiFe_{0.5}Co_{0.5}Ni_{0.5}$ alloys through HEBM in different atmospheres. The results showed that the alloys form BCC structures in Ar atmosphere and exhibit two-step hydrogen absorption, but the inferior hydrogen storage characteristics (only 1.2 wt% hydrogen absorption for 1.5 h) is disappointing. Strozi et al. (2021a) synthesized single-phase BCC $Mg_{12}Al_{11}Ti_{33}Mn_{11}Nb_{33}$ HEAs with a hydrogen capacity comparable to that of high-melting point BCC HEAs (1.7 wt%) by performing HEBM in an Ar atmosphere for 24 h (the alloy XRD results are shown in Figure 4B). Recently, the synthesis of $Mg_{35}Al_{15}Ti_{25}V_{10}Zn_{15}$ alloys with high hydrogen capacity (maximum hydrogen capacity 2.5 wt%) has been reported by using HEBM in Ar atmosphere (Ferraz et al., 2022). The authors concluded that the addition of light elements does not contribute to the formation of solid solution phase nor the weight hydrogen storage capacity of the alloy. Moreover, it was discovered that the alloy powder after ball

TABLE 1 Reported BCC-structured HEAs' hydrogen storage performance.

HEA composition	Synthesis and processes	Hydrogen absorption capacity (wt%)	H/M	Hydrogen absorption kinetics	Onset/peak temperature of desorption, °C	Ref
TiVZrNbHf	AM	~2.7	2.5	—	200/400 (TDS)	Zhang et al. (2020)
TiZrNbHf	AM (Ar)	—	~1.95	—	300/400 (TGA/DSC)	Nygård et al. (2019a), Ek et al. (2021)
$Ti_{0.5}VZrNbHf$	AM (Ar)	—	~2.0	—	<400 (TGA/DSC)	Ek et al. (2021)
$TiV_{0.5}ZrNbHf$	AM (Ar)	—	~2.0	—	<400 (TGA/DSC)	Ek et al. (2021)
$Ti_{0.2}Zr_{0.2}Hf_{0.2}Mo_{0.1}Nb_{0.3}$	AM	1.54 (REV)	—	—	332 (TGA/DSC)	Shen et al. (2020)
$Ti_{0.2}Zr_{0.2}Hf_{0.2}Mo_{0.3}Nb_{0.1}$	AM	1.4 (REV)	—	—	164 (TGA/DSC)	Shen et al. (2020)
TiZrHfMoNb	AM	1.18 (REV)	—	—	300 (TGA/DSC)	Shen et al. (2019)
TiZrNbHfTa	AM	—	2.0	—	183 (1st. Peak)	Zlotea et al. (2019)
					375 (2nd. Peak)	
					485 (3rd. Peak) (TDS/DSC)	
$Ti_4V_3NbCr_2$	VAM	3.7	~2.0	3.7 wt% in 150 s (300 K, 50 bar H_2)	423 (DSC)	Cheng et al. (2022)
TiVCrNb	AM (Ar)	1.96 (REV)	~1.9	—	200 (DSC)	Nygård et al. (2019a)
$Al_{0.1}Ti_{0.3}V_{0.25}Zr_{0.1}Nb_{0.25}$	AM	2.6	1.6	~2.6 wt% in 300 s (298 K, 25 bar H_2)	110/130 (1st. Peak)	Montero et al. (2021b)
					286 (2nd. Peak) (TDS)	
$V_{48}Fe_{12}Ti_{30}Cr_{10}$	AM	2.81	—	~2.6 wt% in 140 s (295 K, 5 MPa H_2)	156 (DSC)	Luo et al. (2022)
$(V_{48}Fe_{12}Ti_{30}Cr_{10})_{95}La_5$	AM	~2.3	—	~2.0 wt% in 100 s (295 K, 5 MPa H_2)	273 (DSC)	Luo et al. (2022)
$Mg_{0.1}Ti_{0.3}V_{0.25}Zr_{0.1}Nb_{0.25}$	HEBM (Ar)	2.7	1.72	2.7 wt% in 60 s (298 K, 25 bar H_2)	290 (TDS)	Montero et al. (2021a)
$MgZrTiFe_{0.5}Co_{0.5}Ni_{0.5}$	HEBM (Ar)	1.2	—	1.0 wt% in 30 min (623 K, 2 MPa H_2)	230/300 (1st. Peak)	Zepon et al. (2017)
					375 (Peak) (DSC/QMS)	
$Mg_{13}Al_{11}Ti_{33}Mn_{11}Nb_{33}$	HEBM (Ar)	1.7	1.0	—	—	Strozi et al. (2021a)
$Mg_{35}Al_{15}Ti_{25}V_{10}Zn_{15}$	HEBM (Ar)	2.5	—	2.5 wt% in 4 h (648 K, 4 MPa H_2)	400 (TGA/DSC/QMS)	Ferraz et al. (2022)
$V_{30}Ti_{30}Cr_{25}Fe_{10}Nb_5$	AM (Ar)	2.77	—	—	—	Liu et al. (2021b)
$V_{35}Ti_{30}Cr_{25}Fe_5Mn_5$	AM (Ar)	3.41	—	—	—	Liu et al. (2021b)

Note: Here AM refers to arc melting.

10.3389/fmats.2023.1135864

milling was mixed with Fe impurities, which is very common in HEBM process. The impurities reacting with the alloy will change its phase composition and structure, which may cause degradation of the eventual performance in hydrogen storage.

While classical metallurgical techniques such as VAM and MA are capable of synthesizing individual components, the development of high-throughput techniques for the production and screening of HEAs is more beneficial for exploring their vast compositional design space. Shi et al. (2020) achieved high-throughput synthesis of Al_x $(CoCrFeNi)_{100-x}$ HEA films covered with 4.5–40 at% Al using magnetron co-sputtering. It is inspired that if the properties of the corresponding hydrides can be simultaneously characterised, it will greatly facilitate the high-throughput design of HEAs for hydrogen storage. Moorehead et al. (2020) showed that *in situ* alloying of different elements through additive manufacturing could explore HEA space in a high-throughput manner, saving one order of magnitude in time compared to arc melting. However, there are deviations between the predetermined composition of the system and the actual composition of the additive manufacturing alloy, for which further optimization is needed. Although the method of synthesizing HEAs in a high-throughput manner still needs to be studied in depth, it brings new hope to improve the efficiency of research and development of new HEAs for hydrogen.

4 Hydrogen storage properties of BCC-structured HEAs

BCC HEAs have been widely studied in solid-state hydrogen storage, and many alloy compositions with excellent performance have been discussed as summarized in Table 1. We will discuss the hydrogen storage properties of BCC-structured high-entropy alloys separately in the following.

Through Table 1 we note that most combinations of high melting point elements can have hydrogen-to-metal ratios of 2 or even higher. We consider that the TiVCr system HEAs is the most promising alloy for hydrogen storage because it exhibits a rather high hydrogen capacity and rapid hydrogenation kinetic properties. Meanwhile, the arc melting method is the mainstream synthesis method for refractory alloys, which is more helpful for alloy homogeneity and solid solution structure retention.

4.1 Hydrogen capacity

For most BCC alloys, the hydrogen-to-metal ratio can reach 2 or even higher. In this paper, we used weight percent (wt%) as the standard unit of hydrogen capacity. Sahlberg et al. (2016) selected compositional combinations of Ti, V, Zr, Nb, and Hf as pure hydrogen-absorbing elements to synthesize the BCC HEA. The peculiarity of this work is that the alloy achieves a hydrogen-to-metal ratio of 2.5, but only corresponds to 2.7 wt% because of the high molecular weight of the selected elements. Their results show that the tetrahedral and octahedral sites of the alloy are filled with hydrogen at the same time, which is coupled with large lattice distortions and explained this large hydrogen-to-metal ratio. Unfortunately, the TiZrNbHfTa alloy, also synthesized from pure hydrogen-absorbing elements in their subsequent work (Zlotea et al., 2019), did not show similar hydrogen-absorbing properties and only reached a capacity of H/M = 2. Zepon et al. (2017) developed a BCC single-phase $MgZrTiFe_{0.5}Co_{0.5}Ni_{0.5}$ alloy and the hydrogen capacity was 1.2 wt%. Their subsequent work synthesised $Mg_{12}Al_{11}Ti_{33}Mn_{11}Nb_{33}$ alloy with 1.75 wt% hydrogen capacity (Strozi et al., 2021a). Pineda-Romero and Zlotea (2022) discussed the effect of Al addition (from small to equimolar ratios) on the hydrogen storage behaviour of TiVNb alloys and concluded that increasing Al content decreases the hydrogen capacity of the alloy. These reports indicate that the addition of lightweight elements does not necessarily have a significant enhancement effect on the hydrogen storage weight capacity of the alloy. In a work by the presented authors, it is reported that the $Ti_4V_3NbCr_2$ HEA possesses a hydrogen capacity of 3.7 wt%, and to the best knowledge of the authors, this is the highest hydrogen capacity reported for BCC-structured HEA currently.

4.2 Activation

In most cases, the BCC structure alloys need to be activated through hydrogen absorption/desorption cycles at high temperature and high pressure to achieve hydrogen absorption at room temperature. Zhang et al. (2020) found that the hydrogen absorption temperature of TiZrNbTa alloy decreased substantially (715 K–300 K) after three hydrogen absorption/desorption cycles at high temperature (1073 K hydrogen absorption as well as 1123 K desorption). The authors proposed a two-step activation mechanism of surface oxide reduction to suboxide and suboxide conversion to subhydroxide for explaining the activation. They suggested that sub-hydroxide formation is more important than the effect of suboxides on the activation and hydrogen absorption temperature of HEAs, and the reason is the easy diffusion of hydrogen atoms inside sub-hydroxides. Sleiman and Huot (2021) investigated the effects of particle size, pressure and temperature on the activation of TiVZrHfNb alloy, where the effect of temperature on activation was more pronounced and no hydrogen was absorbed even after 24 h exposure to hydrogen atmosphere at temperatures below 200°C. The authors suggest that this is consistent with the Arrhenius mechanism and use it to help understand the incubation period for the first hydrogenation of the alloy. Xue et al. (2023) improved the activation of TiVCr alloy by adding Ce element. As an element with high oxygen affinity, Ce can prevent oxidation of other components on the alloy surface and reduce the activation difficulty of it. This work provides a new idea for the activation of BCC high-entropy hydrogen storage alloys, but the drawback is that Ce does not react with H, which adversely influences the hydrogen storage capacity. The appropriate amount of addition is the main challenge of this approach, and the composition design based on the computational method may help and save the large material consumption accompanying the trial-and-error experiments. Furthermore, some alloys with simple activation conditions have also been reported. Liu et al. (2022b) reported that after the sample of $V_{0.3}Ti_{0.3}Cr_{0.25}Mn_{0.1}Nb_{0.05}$ alloy was pumped at 373 K for 30 min, the first hydrogenation could absorb 3.45 wt% of hydrogen without incubation time at room temperature and 2 MPa hydrogen pressure.

4.3 Hydrogenation kinetics

The hydrogenation kinetics of HEAs is commonly described as the elapsed time for the alloy to reach 90% of its full hydrogen storage capacity. Zhang et al. (2020) concluded that the kinetic data of TiZrNbTa alloys remain consistent with the Johnson-Mehl-Avrami (JMA) equation, which

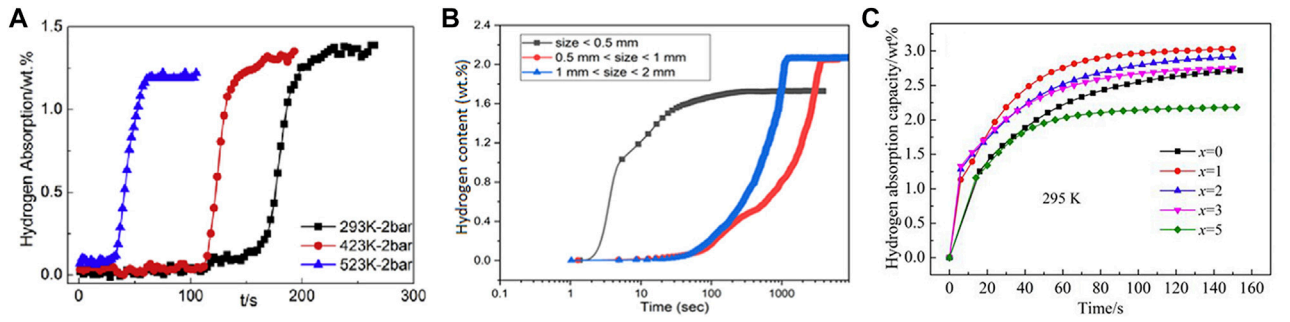

FIGURE 5
Hydrogenation kinetics of TiZrNbTa alloy at different temperatures **(A)** (Zhang et al., 2020); kinetic curves of TiVZrHfNb alloy with different particle sizes at 300°C **(B)** (Sleiman and Huot, 2021); kinetic curves of $(V48Fe12Ti30Cr10)_{100-x}La_x$ alloy with different La additions **(C)** (Luo et al., 2022).

suggests that the hydrogenation kinetics can be interpreted through nucleation and growth mechanisms. HEAs are usually accompanied by large lattice defects and tend to retain vacancy clusters that are difficult to annihilate, and Zhang suggested that these vacancy clusters are responsible for the enhanced hydrogen absorption kinetics after alloy activation, which reduces H-atom diffusion distances or changes diffusion pathways and serves as preferential nucleation sites for hydrides. Although the mechanism of hydrogenation kinetics enhancement (after activation) is interpreted in this work, it is obviously uncontrollable and does not lend itself to a planned upgrading of the hydrogenation kinetics. Sleiman and Huot (2021) have shown that particle size is an important factor affecting the kinetics of alloy hydrogenation. In their work, alloys with small particle sizes (<0.5 mm) exhibited the fastest kinetics, but an increasing or decreasing correlation between particle size and kinetics was not established, and thus subsequent discussion and research is needed. $(V_{48}Fe_{12}Ti_{30}Cr_{10})_{100-x}La_x$ alloy (x = 0,1,2,3,5) was synthesized and its hydrogen absorption/desorption kinetics was discussed by Luo et al. (2022) The results show that the addition of La element enhances the hydrogen absorption kinetics of the alloy, but the kinetic properties of alloys is not enhanced with increasing La content. Furthermore, it is worth noting that the phase structure of the alloy changes with the addition of La elements, which makes the strengthening mechanism more difficult to interpret. For the hydrogen desorption kinetics, the effect of La element is more complicated with more diverse manifestations at different temperatures. Therefore, this approach is not feasible for improving the hydrogenation kinetics and its effect is still uncertain. Figure 5 shows the hydrogenation kinetic curves of the high entropy alloy for different influencing factors. Some alloys with fast room temperature hydrogenation kinetics have also been identified in exploring the factors influencing hydrogenation kinetics. As Hu et al., 2021b) prepared alloys in the TiVCrFe systems with different Ti/Cr ratios, after an activation treatment of 60 min at 400°C, all alloys could reach hydrogen saturation at ~125 s.

4.4 Hydrogenation thermodynamics

The calculation of alloy thermodynamic parameters (ΔH, ΔS) from PCT curves with Van't Hoff equation is widely accepted, although the actual tested PCT curves have a large deviation from the ideal isotherm shape. Zepon et al. (2021) proposed a thermodynamic model that allows the calculation of PCT curves for HEAs, and it was validated by alloys such as TiZrNbHfTa. The authors emphasized the importance of evaluating the sites occupied by hydrogen atoms in the interstial sites of the multicomponent alloys to improve the accuracy of PCT calculations. Pedroso et al. (2022) revalidated this thermodynamic model for calculating PCT curves and developed an open source code with a user-friendly interface as an effective design tool for rapid screening of massive alloys, improving the efficiency of research in the development of new alloys. Kim et al. (2022) used three different ML methods, such as random forest, K-nearest neighbour and deep neural network (DNN), to predict the PCT curves of AB2-type hydrogen storage alloys and proposed a new method of fitting experimental data, which uses the fitting equation of PCT curves to increase the number of PCT data points. It helps to improve the prediction accuracy substantially.

In most reports, overly stable hydrides are considered to account for the difficulty in hydrogen desorption in HEAs with BCC structure. As reported by Nygård et al. (2019a) for alloys with a two-step hydrogen absorption/desorption reaction, alloying affects the kinetic properties of the first step reaction, while the second step reaction needs to be interpreted thermodynamically. They concluded that alloys with higher VEC form more unstable hydrides. Shen et al. (2020) synthesised TiZrHfMoNb system alloys with different Mo contents, and in this work, the desorption temperature of hydrides experienced a significant decrease from 383°C to 164°C as the Mo content increased from 0% to 27%. The authors suggested that this correlation may be due to a decrease in the radius of the interstitial site housing the H atom due to the change in composition, making it more difficult for H to be absorbed and reach the tetrahedral interstitial or octahedral sites of the TiZrHfMoNb cell. The binding energies and enthalpies of formation of the alloy hydrides were obtained by DFT calculations, confirming that changes in Mo content can weaken the bonding of the alloy to H atoms, leading to a decrease in the thermal stability of hydrides. Hu et al. (2021a) investigated the hydrogen storage properties of TiZrVMoNb HEA by the DFT method, and the combined energy and generation enthalpy calculations showed that tetrahedral interstitial hydrogen occupancy improves FCC hydride stability, but additional octahedral occupancy can break this stability, which provides a new pathway to reduce the difficulty of hydrogen desorption in BCC-structured HEAs. Although the addition of alloying elements can effectively reduce the enthalpy of decomposition of alloy hydrides, the amount of alloying elements added, the atomic size and the difficulty of binding the elements to hydrogen may affect the final results. This makes the modulation

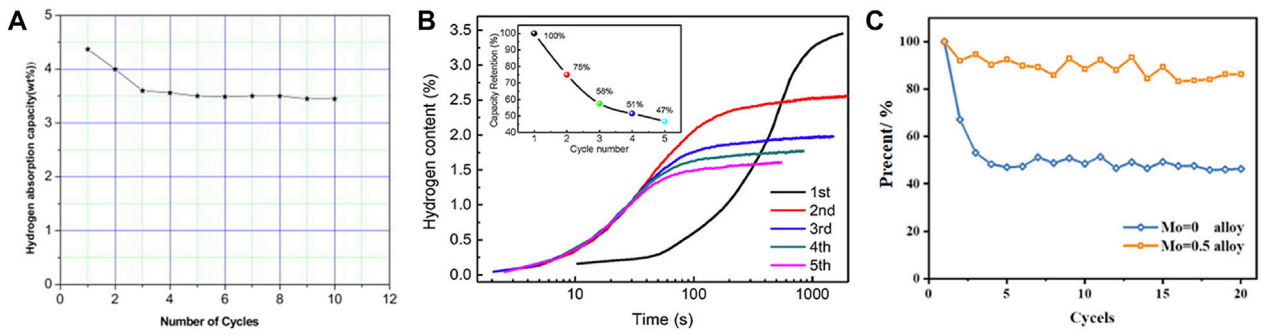

FIGURE 6
Hydrogen capacity of Ti_2VCr alloy for 10 cycles at room temperature (the alloy is heated at 673 K under diffusion vacuum before each cycle) **(A)** (Kumar et al., 2011); hydrogen absorption curve of $V_{0.3}Ti_{0.3}Cr_{0.25}Mn_{0.1}Nb_{0.05}$ alloy within 5 cycles **(B)** (Liu et al., 2022b); comparison of cycling performance of Ti2VCr alloy before and after chemical modification (Mo instead of Ti) **(C)** (Hu et al., 2022).

process full of uncertainties. Therefore, we consider that options with higher pervasiveness are also needed. Recently, Strozi et al. (2021b) synthesized a TiVNbCr system alloy by varying the Cr ratio and found that the hydride stability of the alloy decreases with increasing Cr content. Since Cr contributes to the formation of the C15 Laves phase, this unsurprisingly leads to a decrease in the maximum hydrogen storage capacity. On the other hand, there is a threshold for a significant decrease in hydrogen storage capacity between 35% and 40% Cr content, suggesting that there is an upper limit to the amount of Cr addition to retain at least 2 wt% of reversible hydrogen storage capacity. It is noted that in other reports, the active trace introduction of secondary phases has shown good results in improving hydrogenation kinetics and hydride stability, although this comes at the expense of some hydrogen capacity. For most applications, compositions with better reversible hydrogen storage capacity are more valuable than high hydrogen capacity alone, which may introduce a broader approach to performance tuning.

4.5 Cycling property

The critical aspect of investigating its cyclic performance is to mitigate the cyclic decay of the effective hydrogen storage capacity, in consideration of the two-step hydrogen absorption/desorption characteristics for BCC HEA. Previously, Kumar et al. (2011) discovered that the Ti_2VCr alloy shows maximum hydrogen storage capacity of 4.37 wt% at room temperature, but decreased about 20% after three cycles, even though hydrogen was released at 400°C after each cycle (as shown in Figure 6A). To solve this problem, the Ti2VCr alloy was modified by introducing more non-hydrogen absorbing elements. Liu et al. (2022b) showed that the $V_{0.3}Ti_{0.3}Cr_{0.25}Mn_{0.1}Nb_{0.05}$ BCC HEA resulted in a more severe decay of hydrogen absorption if it was not released at high temperature after cycling, and the third cycle only reaches about 60% of the first hydrogen absorption (as shown in Figure 6B). As the number of cycles increases, the effective hydrogen release of the alloy stabilizes at about 1.5 wt%. This may be attributed to the fact that the first hydrogen absorption plateau of the alloy generates stable monohydrides and only a small portion of hydrogen is involved in the hydrogen absorption and release cycle in the subsequent process. In this work, the effective hydrogen storage is even lower than 50% of the maximum hydrogen absorption, the mechanism of which remains to be uncovered. Hu et al. (2022) synthesized $Ti_{1.5}Mo_{0.5}CrV$ alloy by Mo substitution of Ti with better cyclic stability than Ti_2CrV which showed nearly half loss of hydrogen absorption at the beginning of cycling (as shown in Figure 6C). The authors suggested that Mo doping could stabilize the crystal structure of the alloy to avoid serious lattice defects and deformation after hydrogen absorption and desorption, and achieve the purpose of stabilizing the cyclic performance of the alloy. However, it should be noted that this approach may not be applicable to stabilize the cyclic performance of HEAs with five elements or higher alloying levels, where the lattice defects are already severe. Montero et al. (2021a) improved the hydrogen cycling performance of TiVNbZr HEA by adding Mg, which stabilized the reversible hydrogen storage from the second cycle, only having a slight decay from 2.7 wt% to 2.4 wt%. The authors concluded that good compositional homogeneity is a key factor in the enhanced cycling performance of the alloy. Several reports have been published on the reasons for the capacity decay that occurs during cycling. Wan et al. (2009) reported the changes in the crystal structure and chemical state of TiCrVMn alloy after different times of hydrogen absorption/desorption cycles. The authors concluded that the alloy may develop lattice defects and shrink the lattice volume after hydrogen absorption/desorption. This change leads to a decrease in hydrogen occupancy sites, exhibiting a decay in hydrogen capacity with increasing number of cycles. Meanwhile, Wan suggested that the passivated composite oxide film formed due to the absorption of impurities in hydrogen by the surface metal is important in inhibiting the hydrogenation reaction. Luo et al. (2015) suggested that smaller grain size is more prone to release micro-stress and reduce micro-strain in the lattice, which is more helpful in maintaining the capacity of the alloy during hydrogen absorption/desorption cycles. It should be noted that when the alloy grain size is less than 25 μm, it is more susceptible to impurity gases, leading to a decrease in the durability of the absorption/desorption cycle.

5 Potential applications for BCC-structured HEAs

Currently, BCC-structured HEAs show excellent hydrogen storage properties such as high hydrogen capacity, fast kinetics, high

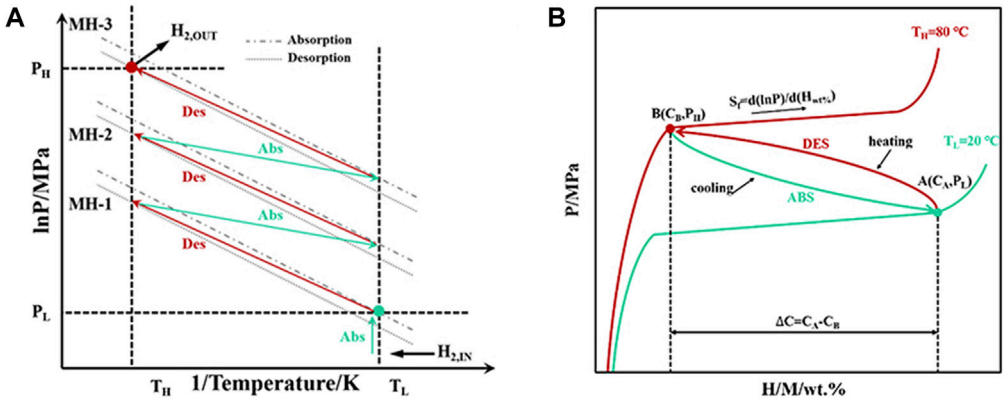

FIGURE 7
Schematic diagram of a three-stage hydrogen compressor **(A)**; and working principle of hydrogen compression materials **(B)** (Peng et al., 2021).

temperature stability, and reliable cycling stability, with differences in performance focus for different application directions. Possible application scenarios are described as follows.

5.1 Explosives or solid propellants

Enhancing the combustion and explosive performance of explosives or solid propellants through the addition of metal hydrides has been recognized in many studies, in which AlH3 is considered as a potential alternative to Al mixed in solid propellants because AlH3 fuels possess a higher specific impulse compared to Al fuels at the same mass fraction (Liu et al., 2021a). In addition, some other metal hydrides have also been reported as additives for explosives and solid propellants, such as MgH2 with high ignition sensitivity, ZrH2 to promote the combustion efficiency of propellants, and TiH2 with high storage stability (Yang et al., 2020; Wu et al., 2020). A great number of reports have confirmed that the BCC phase is more favourable for hydrogen storage, and the process of preparing single phase HEAs containing lighter elements (such as Mg,Al, etc.) has also been published. We suggest that the hydride of BCC-structured HEA is expected to be an efficient additive for explosives or solid propellants. In addition, due to the specificity of the application, the cyclic and reversible properties of the hydrogenation are not considered. While counting the high degree of freedom on the cost of the alloy, these factors greatly reduce the difficulty of alloy composition design which accelerates the development efficiency of high hydrogen capacity HEAs.

5.2 Hydrogen transportation industry

Hydrogen storage alloys are the pillars of hydrogen energy industry development and can be involved in hydrogen storage, transportation and refuelling. BCC HEAs are promising materials for hydrogen storage and transportation, which combine high reversible hydrogen storage capacity with suitable thermodynamic properties for efficient and safe hydrogen storage and transportation. In the construction of hydrogen refuelling stations, hydrogen compressors play a central role. Peng et al. (2021) reported a design scheme of a three-stage metal hydride hydrogen compressor employing graded compression to achieve high output pressure of hydrogen, and discussed the performance requirements of hydrogen compression materials. The authors suggested that a suitable hydrogen compression material needs to have a plateau pressure matching the input/output side of the compressor (as shown in Figure 7), which is a prerequisite for achieving hydrogen compression. The compression efficiency is determined by the reversible hydrogen storage capacity and kinetic performance. Furthermore, the material needs to have resistance to poisoning effect from impurity gases and strong cycling stability for a long term use. Based on the published reports, the composition design of BCC-structured HEAs can easily achieve the requirements of plateau pressure and compression efficiency, but the resistance to poisoning and cycling properties of the alloy need to be further improved (Sahlberg et al., 2016; Sleiman and Huot, 2021; Hu et al., 2021a; Montero et al., 2021a; Ulmer et al., 2018).

5.3 Grid energy storage and high temperature thermal storage

Renewable energy sources (e.g. solar, wind, tidal, etc.) are increasingly penetrating microgrids and district power supply systems, but their intermittent and uncontrollable characteristics are a serious challenge for large-scale application (Seane et al., 2022; Bunker and Weaver, 2018; Petreus et al., 2019). BCC HEAs are expected to be an important component of grid energy storage systems for their high hydrogen capacity, stable hydrides, and stable cycling, and stable output of electricity through the conversion of renewable energy to hydrogen. The high thermal stability of alloy hydrides ensures a safer energy storage system. A further problem that requires attention is the introduction of large amounts of heat energy for hydrogen release, which causes additional energy losses. Additionally, the application requires a long-term repetition of the hydrogen absorption/desorption process, which places higher demands on the cycling performance of the alloy, while the large-scale usage of materials makes the cost issue to be considered.

The research of high-temperature thermal storage materials is classified into sensible heat storage, latent heat storage and thermochemical heat storage materials according to different heat

storage pathways. The thermochemical energy storage through the reversible reaction of metal and hydrogen has been reported for long, such as MgH which achieves reversible thermochemical high-temperature thermal storage at 500°C with excellent thermal storage capacity (0.6–0.7 kWh/kg Mg). Shen et al. (2019) reported a TiZrHfMoNb high-entropy alloy for solar thermal energy storage and concluded that the reversible single-phase transformation during hydrogen absorption/desorption improves the hydrogen recovery rate and energy efficiency. Actually, a large portion of the BCC-structured HEAs has high generation enthalpy and hydrogen capacity with great potential for thermal storage applications. Moreover, a combination of high enthalpy alloy for heat storage and low enthalpy alloy for hydrogen storage has been proposed to solve the hydrogen storage problem when the hydrogen storage alloy is applied to high temperature heat storage systems. The disadvantage of this idea is that the complex conversion process is very prone to energy loss and the cost of the alloy is a heavy burden for its implementation.

6 Conclusion

BCC-structural HEAs offer more possibilities for the development of hydrogen storage materials with great potential for hydrogen storage in application. From this investigation, the conclusions we obtained are shown as follows:

1. The composition design of BCC-structured HEAs for hydrogen storage will increasingly rely on computational methods, especially based on the expected properties to down-select the promising compositions.
2. A suitable preparation process can stabilize the BCC structure of HEA, which is more conducive to the investigation of its hydrogen storage properties.
3. Almost all hydrogen storage alloys with high hydrogen capacity face the challenge of difficult hydrogen desorption, so reducing the temperature of hydrogen desorption and improving the cyclic performance of the alloy will be the main future development direction for the hydrogen storage performance of BCC-structured HEAs.
4. More or less shortcomings in the performance of BCC-structured HEAs are reported as “potential materials” in many application scenarios, which makes the rapid research and development methods of their active ingredients increasingly important.

Author contributions

LK, BC, and DW contributed to conception and design of the study. LK and BC organized the database. LK wrote the first draft of the manuscript. BC, DW, and YX wrote sections of the manuscript. DW and YX supervised the study. All authors contributed to manuscript revision, read, and approved the submitted version.

Funding

This research was funded by Graduate Interdisciplinary Innovation Project of Yangtze Delta Region Academy of Beijing Institute of Technology (Jiaxing), No. GIIP 2022-012.

Conflict of interest

The authors declare that the research was conducted in the absence of any commercial or financial relationships that could be construed as a potential conflict of interest.

Publisher’s note

References

Bunker, K., and Weaver, W. (2018). Optimal multidimensional droop control for wind resources in DC microgrids. *Energies* 11 (7), 1818. doi:10.3390/en11071818

Cantor, B., Chang, I. T. H., Knight, P., and Vincent, A. J. B. (2004). Microstructural development in equiatomic multicomponent alloys. *Mater. Sci. Eng. A* 375-377, 213–218. doi:10.1016/j.msea.2003.10.257

Cheng, B., Wan, D., Wang, B., Xue, Y., Wang, L., Cao, T., et al. (2022). Solid-state hydrogen storage properties of Ti–V–Nb–Cr high-entropy alloys and the associated effects of transitional metals (M = Mn, Fe, Ni). *Acta Metall. Sin. Engl. Lett.* doi:10.1007/s40195-022-01403-9

Dashbabu, D., Kumar, E. A., and Jain, I. P. (2022). Thermodynamic analysis of a metal hydride hydrogen compressor with aluminium substituted LaNi5 hydrides. *Int. J. Hydrogen Energy*. doi:10.1016/j.ijhydene.2022.09.094

Edalati, P., Floriano, R., Mohammadi, A., Li, Y., Zepon, G., Li, H. W., et al. (2020). Reversible room temperature hydrogen storage in high-entropy alloy TiZrCrMnFeNi. *Scr. Mat.* 178, 387–390. doi:10.1016/j.scriptamat.2019.12.009

Ek, G., Nygård, M. M., Pavan, A. F., Montero, J., Henry, P. F., Sorby, M. H., et al. (2021). Elucidating the effects of the composition on hydrogen sorption in TiVZrNbHf-based high-entropy alloys. *Inorg. Chem.* 60 (2), 1124–1132. doi:10.1021/acs.inorgchem.0c03270

Ferraz, M. D. B., Botta, W. J., and Zepon, G. (2022). Synthesis, characterization and first hydrogen absorption/desorption of the Mg35Al15Ti25V10Zn15 high entropy alloy. *Int. J. Hydrogen Energy* 47 (54), 22881–22892. doi:10.1016/j.ijhydene.2022.05.098

Garcés, J. (2010). The configurational entropy of mixing of interstitials solid solutions. *Appl. Phys. Lett.* 96, 161904. doi:10.1063/1.3400221

Guo, S., Ng, C., Lu, J., and Liu, C. T. (2011). Effect of valence electron concentration on stability of fcc or bcc phase in high entropy alloys. *J. Appl. Phys.* 109, 103505. doi:10.1063/1.3587228

Guo, W., Dmowski, W., Noh, J. Y., Rack, P., Liaw, P. K., and Egami, T. (2013). Local atomic structure of a high-entropy alloy: An X-ray and neutron scattering study. *Metall. Mat. Trans. A* 44, 1994–1997. doi:10.1007/s11661-012-1474-0

Hu, J., Shen, H., Jiang, M., Gong, H., Xiao, H., Liu, Z., et al. (2019). A DFT study of hydrogen storage in high-entropy alloy TiZrHfScMo. *Nanomater. (Basel)* 9 (3), 461. doi:10.3390/nano9030461

Hu, J., Zhang, J., Xiao, H., Xie, L., Sun, G., Shen, H., et al. (2021). A first-principles study of hydrogen storage of high entropy alloy TiZrVMoNb. *Int. J. Hydrogen Energy* 46 (40), 21050–21058. doi:10.1016/j.ijhydene.2021.03.200

Hu, H., Ma, C., and Chen, Q. (2021). Mechanism and microstructural evolution of TiCrVFe hydrogen storage alloys upon de-/hydrogenation. *J. Alloys Compd.* 877, 160315. doi:10.1016/j.jallcom.2021.160315

Hu, H., Ma, C., and Chen, Q. (2022). Improved hydrogen storage properties of Ti2CrV alloy by Mo substitutional doping. *Int. J. Hydrogen Energy* 47 (23), 11929–11937. doi:10.1016/j.ijhydene.2022.01.212

Kim, J. M., Ha, T., Lee, J., Lee, Y. S., and Shim, J. H. (2022). Prediction of pressure-composition-temperature curves of AB2-type hydrogen storage alloys by machine learning. *Mater. Mat. Int.* doi:10.1007/s12540-022-01262-0

Kumar, A., Shashikala, K., Banerjee, S., Nuwad, J., Das, P., and Pillai, C. (2011). Effect of cycling on hydrogen storage properties of Ti2CrV alloy. *Int. J. Hydrogen Energy* 37 (4), 3677–3682. doi:10.1016/j.ijhydene.2011.04.135

Kumar, A., Muthukumar, P., and Kumar, E. A. (2022). Absorption based solid state hydrogen storage system: A review. *Sustain. Energy Technol. Assess.* 52, 102204. doi:10.1016/j.seta.2022.102204

Latroche, M., Baricco, M., Dematteis, E. M., Berti, N., and Cuevas, F. (2021). Substitutional effects in TiFe for hydrogen storage: A comprehensive review. *Mat. Adv.* 2 (8), 2524–2560. doi:10.1039/d1ma00101a

Lebrouhi, B. E., Djoupo, J. J., Kousksou, T., and Benabdelaziz, K. (2022). Global hydrogen development-A technological and geopolitical overview. *Int. J. Hydrogen Energy* 47, 7016–7048. doi:10.1016/j.ijhydene.2021.12.076

Li, C., Gao, X., Yuan, Z., Wei, X., Zhang, W., Lan, Y., et al. (2022). Effects of Zr doping on activation capability and hydrogen storage performances of TiFe-based alloy. *Int. J. Hydrogen Energy* 48, 2256–2270. doi:10.1016/j.ijhydene.2022.10.098

Lin, H. J., Lu, Y. S., Zhang, L. T., Liu, H. Z., Edalati, K., and Revesz, A. (2022). Recent advances in metastable alloys for hydrogen storage: A review. *Rare Met.* 41, 1797–1817. doi:10.1007/s12598-021-01917-8

Liu, Y., Pan, H., Lei, Y., and Zhu, Y. (2004). Hydrogen storage and electrochemical properties of the La0.7Mg0.3Ni3.825-xCo0.675Mnx hydrogen storage electrode alloys. *J. Alloys Compd.* 365, 246–252. doi:10.1016/s0925-8388(03)00642-x

Liu, J., Yuan, J., Li, H., Pang, A., Xu, P., Tang, G., et al. (2021). Thermal oxidation and heterogeneous combustion of AlH3 and Al: A comparative study. *Acta Astronaut.* 179, 636–645. doi:10.1016/j.actaastro.2020.11.039

Liu, J., Xu, J., Sleiman, S., Chen, X., Zhu, S., Cheng, H., et al. (2021). Microstructure and hydrogen storage properties of Ti–V–Cr based BCC-type high entropy alloys. *Int. J. Hydrogen Energy* 46 (56), 28709–28718. doi:10.1016/j.ijhydene.2021.06.137

Liu, H., Zhang, J., Liu, Y., Zhou, C., and Fang, Z. Z. (2022). Effect of oxygen addition on phase composition and activation properties of TiFe alloy. *Int. J. Hydrogen Energy*. doi:10.1016/j.ijhydene.2022.11.353

Liu, J., Xu, J., Sleiman, S., Ravalison, F., Zhu, W., Liu, H., et al. (2022). Hydrogen storage properties of V0.3Ti0.3Cr0.25Mn0.1Nb0.05 high entropy alloy. *Int. J. Hydrogen Energy* 47 (61), 25724–25732. doi:10.1016/j.ijhydene.2022.06.013

Luo, L., Li, Y., Liu, S., Yang, F., Yuan, Z., Li, L., et al. (2022). Nanoscale microstructure and hydrogen storage performance of as cast La-containing V-based multicomponent alloys. *Int. J. Hydrogen Energy* 47 (80), 34165–34182. doi:10.1016/j.ijhydene.2022.08.021

Luo, L., Wu, C., Yang, S., Zhou, J., Chen, Y., Yang, F., et al. (2015). Decaying behaviors of V40(TiCr)51Fe8Mn hydrogen storage alloys with different particle sizes. *J. Alloys Compd.* 645, S178–S183. doi:10.1016/j.jallcom.2014.12.261

Lv, L., Lin, J., Liu, W., Ma, Z., Xu, L., He, X., et al. (2022). Hydrogen storage performance of LaNi3.95Al0.75Co0.3 alloy with different preparation methods. *Prog. Nat. Sci. Mater. Int.* 32, 206–214. doi:10.1016/j.pnsc.2022.02.001

Montero, J., Ek, G., Sahlberg, M., and Zlotea, C. (2021). Improving the hydrogen cycling properties by Mg addition in Ti-V-Zr-Nb refractory high entropy alloy. *Scr. Mat.* 194, 113699. doi:10.1016/j.scriptamat.2020.113699

Montero, J., Ek, G., Laversenne, L., Nassif, V., Sahlberg, M., and Zlotea, C. (2021). How 10 at% Al addition in the Ti-V-Zr-Nb high-entropy alloy changes hydrogen sorption properties. *Molecules* 26 (9), 2470. doi:10.3390/molecules26092470

Moorehead, M., Bertsch, K., Niezgoda, M., Parkin, C., Elbakhshwan, M., Sridharan, K., et al. (2020). High-throughput synthesis of Mo-Nb-Ta-W high-entropy alloys via additive manufacturing. *Mat. Des.* 187, 108358. doi:10.1016/j.matdes.2019.108358

Nygård, M. M., Ek, G., Karlsson, D., Sorby, M. H., Sahlberg, M., and Hauback, B. C. (2019). Counting electrons - a new approach to tailor the hydrogen sorption properties of high-entropy alloys. *Acta Mat.* 175, 121–129. doi:10.1016/j.actamat.2019.06.002

Nygård, M. M., Ek, G., Karlsson, D., Sahlberg, M., Sorby, M. H., and Hauback, B. C. (2019). Hydrogen storage in high-entropy alloys with varying degree of local lattice strain. *Int. J. Hydrogen Energy* 44 (55), 29140–29149. doi:10.1016/j.ijhydene.2019.03.223

Nygård, M. M., Sławiński, W. A., Ek, G., Sorby, M. H., Sahlberg, M., Keen, D. A., et al. (2020). Local order in high-entropy alloys and associated deuterides - a total scattering and Reverse Monte Carlo study. *Acta Mat.* 199, 504–513. doi:10.1016/j.actamat.2020.08.045

Pedroso, O. A., Botta, W. J., and Zepon, G. (2022). An open-source code to calculate pressure-composition-temperature diagrams of multicomponent alloys for hydrogen storage. *Int. J. Hydrogen Energy* 47 (76), 32582–32593. doi:10.1016/j.ijhydene.2022.07.179

Peng, Z., Li, Q., Zhu, M., Jiang, W., Chen, K., Wang, H., et al. (2021). Overview of hydrogen compression materials based on a three-stage metal hydride hydrogen compressor. *J. Alloys Compd.* 895, 162465. doi:10.1016/j.jallcom.2021.162465

Petreus, D., Etz, R., Patarau, T., and Cirstea, M. (2019). An islanded microgrid energy management controller validated by using hardware-in-the-loop emulators. *Int. J. Electr. Power Energy Syst.* 106, 346–357. doi:10.1016/j.ijepes.2018.10.020

Pineda-Romero, N., and Zlotea, C. (2022). Uncovering the effect of Al addition on the hydrogen storage properties of the ternary TiVNb alloy. *Materials* 15 (22), 7974. doi:10.3390/ma15227974

Pradeep, K. G., Tasan, C. C., Yao, M. J., Deng, Y., Springer, H., and Raabe, D. (2015). Non-equiatomic high entropy alloys: Approach towards rapid alloy screening and property-oriented design. *Mater. Sci. Eng. A* 648, 183–192. doi:10.1016/j.msea.2015.09.010

Rohit, G., Santosh, M. S., Kumar, M. N., and Raghavendra, K. (2022). Numerical investigation on structural stability and explicit performance of high-pressure hydrogen storage cylinders. *Int. J. Hydrogen Energy*. doi:10.1016/j.ijhydene.2022.11.154

Rusman, N. A. A., and Dahari, M. (2016). A review on the current progress of metal hydrides material for solid-state hydrogen storage applications. *Int. J. Hydrogen Energy* 41, 12108–12126. doi:10.1016/j.ijhydene.2016.05.244

Sahlberg, M., Karlsson, D., Zlotea, C., and Jansson, U. (2016). Superior hydrogen storage in high entropy alloys. *Sci. Rep.* 6, 36770. doi:10.1038/srep36770

Seane, T. B., Samikannu, R., and Bader, T. (2022). A review of modeling and simulation tools for microgrids based on solar photovoltaics. *Front. Energy Res.* 10, 772561. doi:10.3389/fenrg.2022.772561

Senkov, O. N., Wilks, G. B., Miracle, D. B., Chuang, C., and Liaw, P. (2010). Refractory high-entropy alloys. *Intermetallics* 18, 1758–1765. doi:10.1016/j.intermet.2010.05.014

Senkov, O. N., Senkova, S. V., Miracle, D. B., and Woodward, C. (2013). Mechanical properties of low-density, refractory multi-principal element alloys of the Cr–Nb–Ti–V–Zr system. *Mater. Sci. Eng. A* 565, 51–62. doi:10.1016/j.msea.2012.12.018

Shen, H., Zhang, J., Hu, J., Zhang, J., Mao, Y., Xiao, H., et al. (2019). A novel TiZrHfMoNb high-entropy alloy for solar thermal energy storage. *Nanomaterials* 9 (2), 248. doi:10.3390/nano9020248

Shen, H., Hu, J., Li, P., Huang, G., Zhang, J., Zhang, J., et al. (2020). Compositional dependence of hydrogenation performance of Ti-Zr-Hf-Mo-Nb high-entropy alloys for hydrogen/tritium storage. *J. Mat. Sci. Technol.* 55, 116–125. doi:10.1016/j.jmst.2019.08.060

Shi, Y., Yang, B., Rack, P. D., Guo, S., Liaw, P. K., and Zhao, Y. (2020). High-throughput synthesis and corrosion behavior of sputter-deposited nanocrystalline Al (CoCrFeNi)100-combinatorial high-entropy alloys. *Mat. Des.* 195, 109018. doi:10.1016/j.matdes.2020.109018

Silva, B. H., Zlotea, C., Champion, Y., Botta, W. J., and Zepon, G. (2021). Design of TiVNb-(Cr, Ni or Co) multicomponent alloys with the same valence electron concentration for hydrogen storage. *J. Alloys Compd.* 865, 158767. doi:10.1016/j.jallcom.2021.158767

Sleiman, S., and Huot, J. (2021). Effect of particle size, pressure and temperature on the activation process of hydrogen absorption in TiVZrHfNb high entropy alloy. *J. Alloys Compd.* 861, 158615. doi:10.1016/j.jallcom.2021.158615

Strozi, R. B., Leiva, D. R., Huot, J., Botta, W., and Zepon, G. (2021). An approach to design single BCC Mg-containing high entropy alloys for hydrogen storage applications. *Int. J. Hydrogen Energy* 46 (50), 25555–25561. doi:10.1016/j.ijhydene.2021.05.087

Strozi, R. B., Leiva, D. R., Zepon, G., Botta, W. J., and Huot, J. (2021). Effects of the chromium content in (TiVNb)100-xCrx body-centered cubic high entropy alloys designed for hydrogen storage applications. *Energies* 14 (11), 3068. doi:10.3390/en14113068

Strozi, R. B., Silva, B. H., Leiva, D. R., Zlotea, C., Botta, W., and Zepon, G. (2022). Tuning the hydrogen storage properties of Ti-V-Nb-Cr alloys by controlling the Cr/(TiVNb) ratio. *J. Alloys Compd.* 932, 167609. doi:10.1016/j.jallcom.2022.167609

Ulmer, U., Oertel, D., Diemant, T., Bonatto Minella, C., Bergfeldt, T., Dittmeyer, R., et al. (2018). Performance improvement of V–Fe–Cr–Ti solid state hydrogen storage materials in impure hydrogen gas. *ACS Appl. Mat. Interfaces* 10 (2), 1662–1671. doi:10.1021/acsami.7b13541

Usman, M. R. (2022). Hydrogen storage methods: Review and current status. *Renew. Sustain. Energy Rev.* 167, 112743. doi:10.1016/j.rser.2022.112743

Varalakshmi, S., Kamaraj, M., and Murty, B. S. (2008). Synthesis and characterization of nanocrystalline AlFeTiCrZnCu high entropy solid solution by mechanical alloying. *J. Alloys Compd.* 460 (1-2), 253–257. doi:10.1016/j.jallcom.2007.05.104

Wan, C., Ju, X., Qi, Y., Fan, C., Wang, S., Liu, X., et al. (2009). A study on crystal structure and chemical state of TiCrVMn hydrogen storage alloys during hydrogen absorption-desorption cycling. *Int. J. Hydrogen Energy* 34 (21), 8944–8950. doi:10.1016/j.ijhydene.2009.08.060

Wang, J. Y. (2009). Comparison of hydrogen storage properties of Ti0.37V0.38Mn0.25 alloys prepared by mechanical alloying and vacuum arc melting. *Int. J. Hydrogen Energy* 34 (9), 3771–3777. doi:10.1016/j.ijhydene.2009.02.028

Witman, M., Ek, G., Ling, S., Chames, J., Agarwal, S., Wong, J. C. C., et al. (2021). Data-driven discovery and synthesis of high entropy alloy hydrides with targeted thermodynamic stability. *ChemRxiv*. doi:10.26434/chemrxiv.13697464.v1

Wu, X., Xu, S., Pang, A., Cao, W. g., Liu, D. b., Zhu, X. y., et al. (2020). Hazard evaluation of ignition sensitivity and explosion severity for three typical MH2 (M= Mg, Ti, Zr) of energetic materials. *Def. Technol.* 17 (4), 1262–1268. doi:10.1016/j.dt.2020.06.011

Xue, X., Ma, C., Liu, Y., Wang, H., and Chen, Q. (2023). Impacts of Ce dopants on the hydrogen storage performance of Ti-Cr-V alloys. *J. Alloys Compd.* 934, 167947. doi:10.1016/j.jallcom.2022.167947

Yang, X., Chen, S. Y., Cotton, J. D., and Zhang, Y. (2014). Phase stability of low-density, multiprincipal component alloys containing aluminum, magnesium, and lithium. *JOM* 66, 2009–2020. doi:10.1007/s11837-014-1059-z

Yang, Y., Zhao, F., Huang, X., Zhang, J., Chen, X., Yuan, Z., et al. (2020). Reinforced combustion of the ZrH2-HMX-CMDB propellant: The critical role of hydrogen. *Chem. Eng. J.* 402, 126275. doi:10.1016/j.cej.2020.126275

Yeh, J. W., Chen, S. K., Lin, S. J., Gan, J. Y., Chin, T. S., Shun, T. T., et al. (2004). Nanostructured high-entropy alloys with multiple principal elements: Novel alloy design concepts and outcomes. *Adv. Eng. Mater* 6, 299–303. doi:10.1002/adem.200300567

Yin, Y., Li, B., Zhang, Y., and Qi, Y. (2018). Microstructure and hydrogen storage properties of Mg-based Mg 85Zn 5Ni 10 alloy powders. *J. Iron Steel Res. Int.* 25, 1172–1178. doi:10.1007/s42243-018-0177-1

Zepon, G., Leiva, D. R., Strozi, R. B., Bedoch, A., Figueroa, S., Ishikawa, T., et al. (2017). Hydrogen-induced phase transition of MgZrTiFe0.5Co0.5Ni0.5 high entropy alloy. *Int. J. Hydrogen Energy* 43 (3), 1702–1708. doi:10.1016/j.ijhydene.2017.11.106

Zepon, G., Silva, B. H., Zlotea, C., Botta, W. J., and Champion, Y. (2021). Thermodynamic modelling of hydrogen-multicomponent alloy systems: Calculating pressure-composition-temperature diagrams. *Acta Mat.* 215, 117070. doi:10.1016/j.actamat.2021.117070

Zhang, Y., Zhou, Y. J., Lin, J. P., Chen, G., and Liaw, P. (2008). Solid-solution phase formation rules for multi-component alloys. *Adv. Eng. Mat.* 10, 534–538. doi:10.1002/adem.200700240

Zhang, C., Song, A., Yuan, Y., Wu, Y., Zhang, P., Lu, Z., et al. (2020). Study on the hydrogen storage properties of a TiZrNbTa high entropy alloy. *Int. J. Hydrogen Energy* 45, 5367–5374. doi:10.1016/j.ijhydene.2019.05.214

Zhang, Y., Qi, Y., Guo, S., Guo, S. h., and Zhao, D. l. (2022). Research progress of TiFe-based hydrogen storage alloys. *J. Iron Steel Res. Int.* 29, 537–551. doi:10.1007/s42243-022-00756-w

Zhao, W., Ma, J., Zhang, W., and Li, Y. (2022). Potential hydrogen market: Value-added services increase economic efficiency for hydrogen energy suppliers. *Sustainability* 14, 4804. doi:10.3390/su14084804

Zlotea, C., Sow, M. A., Ek, G., Couzinie, J. P., Perriere, L., Guillot, I., et al. (2019). Hydrogen sorption in TiZrNbHfTa high entropy alloy. *J. Alloys Compd.* 775, 667–674. doi:10.1016/j.jallcom.2018.10.108

Zlotea, C., Bouzidi, A., Montero, J., Ek, G., and Sahlberg, M. (2022). Compositional effects on the hydrogen storage properties in a series of refractory high entropy alloys. *Front. Energy Res.* 10, 991447. doi:10.3389/fenrg.2022.991447